

# Dust evolution processes in normal galaxies at $z > 6$ detected by ALMA

Wei-Chen Wang<sup>1,2</sup>, Hiroyuki Hirashita<sup>1</sup> and Kuan-Chou Hou<sup>1,3</sup>

<sup>1</sup>*Institute of Astronomy and Astrophysics, Academia Sinica, PO Box 23-141, Taipei 10617, Taiwan*

<sup>2</sup>*Department of Mechanical Engineering, National Taiwan University, Taipei 10617, Taiwan*

<sup>3</sup>*Department of Physics, Institute of Astrophysics, National Taiwan University, Taipei 10617, Taiwan*

22 November 2016

## ABSTRACT

Recent ALMA observations of high-redshift normal galaxies have been providing a great opportunity to clarify the general origin of dust in the Universe, not biased to very bright special objects even at  $z > 6$ . To clarify what constraint we can get for the dust enrichment in normal galaxies detected by ALMA, we use a theoretical model that includes major processes driving dust evolution in a galaxy; that is, dust condensation in stellar ejecta, dust growth by the accretion of gas-phase metals, and supernova destruction. Using the dust emission fluxes detected in two normal galaxies at  $z > 6$  by ALMA as a constraint, we can get the range of the time-scales (or efficiencies) of the above mentioned processes. We find that if we assume extremely high condensation efficiency in stellar ejecta ( $f_{\text{in}} \gtrsim 0.5$ ), rapid dust enrichment by stellar sources in the early phase may be enough to explain the observed ALMA flux, unless dust destruction by supernovae in those galaxies is stronger than that in nearby galaxies. If we assume a condensation efficiency expected from theoretical calculations ( $f_{\text{in}} \lesssim 0.1$ ), strong dust growth (even stronger than assumed for nearby galaxies if they are metal-poor galaxies) is required. These results indicate that the normal galaxies detected by ALMA at  $z > 6$  are biased to objects (i) with high dust condensation efficiency in stellar ejecta, (ii) with strong dust growth in very dense molecular clouds, or (iii) with efficient dust growth because of fast metal enrichment up to solar metallicity. A measurement of metallicity is crucial to distinguish among these possibilities.

**Key words:** dust, extinction — galaxies: evolution — galaxies: high-redshift — galaxies: ISM — submillimetre: galaxies

## 1 INTRODUCTION

Dust grains in the interstellar medium (ISM) play an important role in radiative and chemical processes. Dust absorbs stellar light and re-emits it in the far infrared (FIR), thus affecting the spectral energy distribution (SED) of a galaxy (e.g. Yajima et al. (2015); Schaerer et al. (2015), for recent modeling). Dust also activates  $\text{H}_2$  formation since the dust surface serves as a reaction site of  $\text{H}_2$  formation (Gould & Salpeter 1963). In addition, since dust is composed of metals (silicon, carbon, oxygen, iron, etc.), it traces the metal enrichment in galaxies (Lisenfeld & Ferrara 1998; Dwek 1998). Therefore, the understanding of dust enrichment in galaxies is of fundamental importance in clarifying the evolutions of galaxies and the interstellar medium.

Galaxies are enriched with metals as a result of their star formation activities. When supernovae (SNe) and asymptotic giant branch (AGB) star winds inject metals in the ISM, a fraction of the metals are condensed into dust

(Kozasa et al. 1989; Todini & Ferrara 2001; Nozawa et al. 2003; Bianchi & Schneider 2007; Gall et al. 2011). Above a certain metallicity level (typically  $\approx 0.1Z_{\odot}$ ), grain growth by the accretion of gas phase metals in the dense ISM becomes the dominant source of dust (Dwek 1998; Hirashita 1999; Inoue 2003; Zhukovska et al. 2008; Valiante et al. 2011; Inoue 2011; Mattsson & Andersen 2012; Asano et al. 2013). This process is referred to as ‘accretion’ in this paper. Furthermore, supernova shocks destroy the dust by sputtering (Dwek & Scalo 1980; Nozawa et al. 2006). In this paper, we consider those processes since they dominate the increase or decrease of the dust mass in a galaxy. Indeed, the models including these processes are successful in reproducing the evolution of dust content as a function of metallicity (Kuo et al. 2013; Rémy-Ruyer et al. 2014; de Bressan et al. 2014). However, applications of dust enrichment models have been limited to bright objects at high

redshift especially at  $z > 5$ , since it was extremely difficult to detect dust emission from such distant galaxies.

Recent observations by the Atacama Large Millimetre/submillimetre Array (ALMA) have been providing a new window to the studies of origin and evolution of dust in the Universe. Because of its high sensitivity, ALMA has potential for detection of dust emission from high-redshift ‘normal’ galaxies represented by Lyman break galaxies (LBGs) and Lyman  $\alpha$  emitters (LAEs) at high redshift ( $z \gtrsim 5$ ) (e.g. [Capak et al. 2015](#)). ALMA has expanded the possibility of high- $z$  dust studies, which had been previously limited to very bright objects such as quasars and submillimetre (submm) galaxies. The current frontier of such dust hunting in high- $z$  LBGs and LAEs is  $z > 6$ , where most of the observations ended up with non-detection of dust continuum ([Ouchi et al. 2013](#); [Ota et al. 2014](#); [Maiolino et al. 2015](#); [Schaerer et al. 2015](#); [Bouwens et al. 2016](#); [Aravena et al. 2016](#)). [Watson et al. \(2015\)](#) recently detected a lensed LBG at  $z = 7.5$ , A1689-zD1 (see also [Knudsen et al. 2016](#)). [Willott et al. \(2015\)](#) also reported a firm and a tentative detection of two LBGs at  $z \sim 6$ . These cases provide important clues to the origin and evolution of dust in the Universe.

[Mancini et al. \(2015\)](#) modelled dust evolution in  $z \gtrsim 6$  galaxies. They adopted a cosmological hydrodynamics simulation and apply a dust evolution model that includes dust formation in stellar ejecta, dust growth by accretion, and dust destruction by shocks as post-processing. By assuming a typical accretion time-scale of nearby galaxies (2 Myr at solar metallicity), they compared the calculated redshift evolution dust mass with the observation data of A1689-zD1, finding that the predicted dust mass is too small in comparison with the observation. Thus, they adopted a shorter accretion time-scale as 0.2 Myr to reproduce the observation, concluding that extremely efficient accretion is required. [Michałowski \(2015\)](#) also concluded a necessity of grain growth by accretion for the same object using a much simpler model. Although [Mancini et al. \(2015\)](#)’s model is based on a realistic semi-analytic model, they basically fixed the parameters concerning the dust production and destruction. Since those parameters may be uncertain, it is still worth making an effort of constraining the time-scales and efficiencies of dust production and destruction using A1689-zD1, in order to quantify how fast each process driving dust evolution works. By modeling this object, we can also address the reason for the non-detection of most sources at  $z > 6$ . In other words, we will be able to clarify what kind of dust evolution process determines the detection and non-detection by ALMA. Thus, the predictions in this paper could be useful for the planning and interpretations of future ALMA observations of high- $z$  galaxies.

This paper is organized as follows. In Section 2, we present the dust enrichment model, and explain how we calculate the corresponding dust emission flux. In Section 3, we apply the model to LBGs at  $z > 6$  detected by ALMA. We discuss our results and parameter dependence in Section 4. In Section 5, we give conclusions on ALMA-detected LBGs. We adopt  $(h, \Omega_m, \Omega_\Lambda) = (0.7, 0.3, 0.7)$  for the cosmological parameters.

## 2 METHOD

The purpose of this paper is to constrain the dust enrichment and destruction processes using stellar and dust luminosities of high-redshift ( $z > 6$ ) normal galaxies detected by ALMA. To this aim, we use a simple one-zone chemical evolution model, from which we obtain the evolution of dust mass and stellar mass. Further, we derive the dust temperature by assuming radiative equilibrium of dust. Based on the stellar mass, dust mass, and dust temperature estimated, we further derive the fluxes at rest-frame ultraviolet (UV) and far-infrared (FIR) wavelengths. These fluxes are compared with observational data, which provide constraints to our model. As a consequence, we obtain an insight into the relevant dust enrichment and destruction time-scales (or efficiencies).

### 2.1 Dust Enrichment Model

To put a particular focus on dust formation and destruction, we adopt a simple analytic model in which the galaxy of interest is treated as a single-zone object. We also neglect inflow and outflow for simplicity; that is, the galaxy is treated as a closed box. In reality, dilution of metals and dust would be expected by inflowing gas in the course of galaxy evolution ([Feldmann 2015](#)). We will comment on such a dilution effect later in Section 4.1. The time evolutions of the gas mass ( $M_g$ ), the metal mass ( $M_Z$ ), and the dust mass ( $M_d$ ) are written as ([Hirashita 1999](#))

$$\frac{dM_g}{dt} = -\psi + E, \quad (1)$$

$$\frac{dM_Z}{dt} = -Z\psi + E_Z, \quad (2)$$

$$\frac{dM_d}{dt} = -\mathcal{D}\psi + f_{\text{in}}E_Z - \frac{M_d}{\tau_{\text{SN}}} + \frac{M_d(1 - f_Z)}{\tau_{\text{acc}}}, \quad (3)$$

where  $\psi$  is the star formation rate (SFR),  $E$  is the total ejection rate of stellar ejecta,  $E_Z$  is the total ejection rate of metals in stellar ejecta,  $Z$  is the metallicity (i.e.  $Z \equiv M_Z/M_g$ ),  $\mathcal{D}$  is the dust-to-gas ratio (i.e.  $\mathcal{D} \equiv M_d/M_g$ ),  $f_{\text{in}}$  is the condensation efficiency of metals in stellar ejecta,  $f_Z$  is the mass fraction of metals locked in the dust (i.e.  $f_Z \equiv M_d/M_Z$ ),  $\tau_{\text{acc}}$  is the time-scale of dust growth by accretion, and  $\tau_{\text{SN}}$  is the time-scale of dust destruction by SN shocks.

For the convenience of analytic treatment, we adopt the instantaneous recycling approximation ([Tinsley 1980](#)). The mass ejection rate of stellar ejecta  $E$  and that of metals  $E_Z$  are both proportional to the star formation rate as  $E = \mathcal{R}\psi$ , and  $E_Z = \mathcal{Y}_Z\psi$ , where  $\mathcal{R}$  and  $\mathcal{Y}_Z$  are the returned fraction and metal yield of stars, respectively. We evaluate  $\mathcal{R}$  and  $\mathcal{Y}_Z$  based on equations (8) and (10) in [Inoue \(2011\)](#) and the fitting formulae of remnant mass  $w(m, Z)$  and metal yield  $m_Z(m)$  from the same reference, using  $5M_\odot$  as the turn-off mass. Consequently we obtain  $\mathcal{R} = 0.1644$  and  $\mathcal{Y}_Z = 0.0139$ . These values are not sensitive to the turn-off mass chosen ([Hirashita & Kuo 2011](#)), and the results below are far more sensitive to the parameters directly related to the dust evolution (i.e.  $f_{\text{in}}$ ,  $\tau_{\text{SN}}$ , and  $\tau_{\text{acc}}$ ).

The SFR is assumed to be regulated by a non-changing star formation time-scale,  $\tau_{\text{SF}}$ , as  $\psi \equiv M_g/\tau_{\text{SF}}$ . Since the efficiency of dust growth by accretion is proportional to the metallicity, the accretion time-scale is written by introduc-

ing the dust growth time-scale at solar metallicity,  $\tau_{\text{acc},0}$  as (Hirashita & Kuo 2011; Mancini et al. 2015)

$$\tau_{\text{acc}} = \tau_{\text{acc},0} \left( \frac{Z}{Z_{\odot}} \right)^{-1}. \quad (4)$$

Therefore, under a given condensation efficiency  $f_{\text{in}}$ , the dust evolution is determined by a given time-scale parameter set  $(\tau_{\text{SF}}, \tau_{\text{acc},0}, \tau_{\text{SN}})$ . It is reasonable that the dust accretion time-scale and SN destruction time-scale are scaled with  $\tau_{\text{SF}}$  for the following reasons. SNe occur more often if more stars formed (Dwek & Scalo 1980). More accretion happens if more gas is contained in the dense ISM phase, which also hosts star formation (Hirashita & Kuo 2011). Therefore, we normalize the accretion and SN destruction time-scales to the star formation time-scale by introducing two parameters,  $\zeta_{\text{acc},0}$  and  $\zeta_{\text{SN}}$ , as

$$\tau_{\text{acc},0} = \zeta_{\text{acc},0} \tau_{\text{SF}}, \quad (5)$$

$$\tau_{\text{SN}} = \zeta_{\text{SN}} \tau_{\text{SF}}. \quad (6)$$

Furthermore, if  $t$  is normalized to  $\tau_{\text{SF}}$ , the same time evolution of  $(M_{\text{g}}, M_{\text{Z}}, M_{\text{d}})$  is obtained as a function of  $t/\tau_{\text{SF}}$ , for the same values of  $f_{\text{in}}$ ,  $\zeta_{\text{acc},0}$  and  $\zeta_{\text{SN}}$ .

For the initial condition, we adopt  $M_{\text{g}} = M_0$ , and  $M_{\text{Z}} = M_{\text{d}} = 0$ . Since we adopt a closed-box model, the star mass  $M_{\star}$  is estimated as

$$M_{\star}(t) = M_0 - M_{\text{g}}(t). \quad (7)$$

Note that all the masses mentioned above are proportional to the initial total mass  $M_0 = M_{\text{g}}(t=0)$ .

## 2.2 FIR and UV luminosity

Schaerer et al. (2015) derived the following relation between UV magnitude at rest 1500 Å,  $M_{1500}$ , and stellar mass  $M_{\star}$ , from SED fitting to a sample of LBGs, including nebular emission and dust attenuation:

$$\log \left( \frac{M_{\star}}{M_{\odot}} \right) = -0.45 \times (M_{1500} + 20) + 9.11. \quad (8)$$

This gives a relation between  $M_{\star}$  calculated by our model and  $M_{1500}$ . We convert  $M_{1500}$  to the UV luminosity  $L_{\text{UV}}$  by adopting

$$M_{1500} = -2.5 \log \left( \frac{L_{\text{UV}}}{L_{\odot}} \right) + 5.73, \quad (9)$$

where the reference values of  $M_{1500}$  and  $L_{\text{UV}}$  are taken from Himiko's ones (Ouchi et al. 2013). As a consequence, we get  $L_{\text{UV}}$  using  $M_{\star}$  calculated in our dust evolution model in Section 2.1. Note that  $L_{\text{UV}}$  is almost proportional to  $M_{\star}$ . The estimated  $L_{\text{UV}}$  already includes the effect of attenuation, but the following conclusions are not affected by the treatment of attenuation because of the small attenuation of our sample.

Although the stellar mass is estimated more precisely using data at longer wavelengths, we use UV magnitude for the following reasons. Since LBGs are UV-selected galaxies, they always have data in the rest UV, while the availability of longer-wavelength data depends on how extensively those objects are followed up. More importantly, the above formula is already tested for a sample of LBGs by Schaerer et al. (2015). Their formula is derived by SED fitting including nebular emission to a sample of LBGs at

$z \sim 7$ , which means that their formula is applicable to the galaxies of interest in our present paper. Therefore, we take advantage of their convenient expression to make our formulation analytically manageable. In addition, we compare the stellar masses estimated by the spectral fitting in Watson et al. (2015) and by the formula in Schaerer et al. (2015), and find that they differ by a factor of 1.4. This is small enough, and does not affect our conclusions.

Besides, the dust temperature ( $T_{\text{d}}$ ) necessary to estimate the submm flux is derived from the condition of radiative equilibrium. Assuming that the UV radiation from stars is the dominant heating source of dust in star-forming galaxies (e.g. Buat & Xu 1996), the radiative equilibrium (the balance between the energies absorbed and emitted by a dust grain) is written as (Hirashita et al. 2014)

$$\pi a^2 Q_{\text{UV}} \frac{L_{\text{UV}}}{4\pi R^2} = \int_0^{\infty} 4\pi \kappa_{\nu} \left( \frac{4}{3} \pi a^3 s \right) B_{\nu}(T_{\text{d}}) d\nu, \quad (10)$$

where  $\kappa_{\nu}$  is the dust mass absorption coefficient,  $s$  is the dust material density,  $a$  is the dust grain radius,  $Q_{\text{UV}}$  is the ratio of the absorption cross-section to the geometric cross-section for UV radiation (which we assume to be 1), and  $R$  is the radius of the spatial dust distribution. We adopt a power-law with an index of  $\beta$  for the mass absorption coefficient,  $\kappa_{\nu} = \kappa_{158} (\nu/\nu_{158})^{\beta} \text{ cm}^2 \text{ g}^{-1}$  following (Hirashita et al. 2014), where  $\kappa_{158}$  is the dust mass absorption coefficient at wavelength  $\lambda = 158 \mu\text{m}$ , and  $\nu_{158} = 1.9 \text{ THz}$  is the frequency corresponding to  $\lambda = 158 \mu\text{m}$ . Among the grain species in Hirashita et al. (2014), we adopt graphite:  $\kappa_{158} = 20.9 \text{ cm}^2 \text{ g}^{-1}$ ,  $\beta = 2$ , and  $s = 2.26 \text{ g cm}^{-3}$  with grain radius  $a = 0.1 \mu\text{m}$ . We discuss the dependence on grain properties in Section 4.2.

Since our selected galaxies are located at high redshifts, we also consider heating by the cosmic microwave background (CMB). We use the following equation to correct the dust temperature for the CMB heating at redshift  $z$  (da Cunha et al. 2013):

$$T_{\text{d}}(z) = \left\{ (T_{\text{d}}^{z=0})^{4+\beta} + (T_{\text{CMB}}^{z=0})^{4+\beta} \left[ (1+z)^{4+\beta} - 1 \right] \right\}^{\frac{1}{4+\beta}}, \quad (11)$$

where  $T_{\text{CMB}}^{z=0} = 2.7 \text{ K}$  is the CMB temperature at  $z = 0$  and  $T_{\text{d}}^{z=0}$  is the dust temperature calculated in equation (10). We hereafter denote the corrected dust temperature  $T_{\text{d}}(z)$  as  $T_{\text{d}}$ .

Now, using the dust mass  $M_{\text{d}}$  calculated in Section 2.1 and the dust temperature  $T_{\text{d}}$  obtained above, we can estimate the dust emission flux ( $f_{\text{d},\nu}$ ) at observational frequency  $\nu$  as (e.g. Dayal et al. 2010))

$$f_{\text{d},\nu} = \frac{(1+z) \kappa_{(1+z)\nu} M_{\text{d}} B_{(1+z)\nu}(T_{\text{d}})}{d_L^2}, \quad (12)$$

where  $d_L$  is the luminosity distance (Carroll et al. 1992) of the object. We also estimate the UV flux  $f_{\text{UV}}$  by the following equation:

$$f_{\text{UV}} = \frac{L_{\text{UV}}}{4\pi d_L^2}. \quad (13)$$

We can see that  $f_{\text{d},\nu}$  is proportional to  $M_{\text{d}}$  from equation (12). As mentioned in Section 2.1,  $M_{\text{d}}$  and  $M_{\star}$  are proportional to  $M_0$ . Moreover, as shown above,  $L_{\text{UV}}$  is almost proportional to  $M_{\star}$ . This indicates that both  $f_{\text{d},\nu}$  and  $f_{\text{UV}}$  are

(almost) proportional to  $M_0$ . Thus, to effectively eliminate the dependence on the unknown  $M_0$ , we compare  $\nu f_{d,\nu}/f_{UV}$  with observations. We multiply  $\nu$  to  $f_{d,\nu}$  to make  $\nu f_{d,\nu}/f_{UV}$  dimensionless. Since we adopt frequencies near to the SED peak,  $\nu f_{d,\nu}$  is roughly the total dust emission flux. Also, since a slight dependence on  $M_0$  still remains for  $f_{UV}$  (note that  $L_{UV}$  is not perfectly proportional to  $M_*$ ; see equations 8 and 9), we adopt a specific value of  $M_0 = 3 \times 10^{10} M_\odot$  although this choice does not affect the following discussions.

### 2.3 Observational Data

We compare the calculated  $\nu f_{d,\nu}/f_{UV}$  with observations. As mentioned in the Introduction, we chose normal galaxies at  $z > 6$  (i.e. the current frontier for dust hunting of normal galaxies) identified in the optical with the dust continuum detected. This sample provides us with opportunity to access ‘normal’ galaxies with moderate SFRs  $\sim 10 M_\odot \text{ yr}^{-1}$ , and enables us to derive a more general picture of dust enrichment in the earliest Universe accessible by ALMA, not biased to submm galaxies or QSOs (Mancini et al. 2015). So far, A1689-zD1 (Watson et al. 2015; Knudsen et al. 2016) and CLM1 (Willott et al. 2015) satisfy this criterion. A1698-zD1 is strongly lensed by a factor of 9.5 and the redshift (7.5) is determined by the spectroscopic break feature at the restframe UV wavelengths. The dust continuum of CLM1 at  $z = 6.2$  was tentatively detected at the  $2\sigma$  level by ALMA. Because of the rareness of the sample, we use this flux as detected, keeping in mind that this might overestimate the dust emission (or the efficiency of dust enrichment) in our model. Willott et al. (2015) also reported a more significant detection of dust continuum emission for WMH 5; however, the emitting regions of dust continuum and stars are clearly different in this object, indicating that this object is a merging system between a dusty galaxy and a dust-free galaxy. Therefore, the UV radiation observed is not likely to be the heating source of the dust in this object, which means that our model cannot be applied to it. In Table 1, we list the observational data adopted in this paper.

## 3 RESULTS

### 3.1 Overall behaviour

In Fig. 1, we plot the normalized flux  $\nu f_{d,\nu}/f_{UV}$  versus the normalized time  $t/\tau_{SF}$ . To separate the effect of each process, we fix two parameters in the set  $(f_{in}, \zeta_{acc,0}, \zeta_{SN})$  and change the other in each panel. In Fig. 1a, we observe that the effect of  $f_{in}$  appears at the early stage and that all the cases converge to the same evolution at later times. Thus, we can conclude that dust condensation in stellar ejecta has an influence on the early evolution. This is consistent with the conclusion by Hirashita (1999) that the stellar dust condensation dominates the dust abundance in the early (low-metallicity) stage of galaxy evolution. Besides, from equation (3), we find that dust growth by accretion and SN destruction are dependent on  $M_d$ . Thus, as the dust abundance becomes large, the evolution is determined by these two processes; this is why all the cases with different  $f_{in}$  converge to the same evolution.

In Figs. 1b and c, we show the effect of changing  $\zeta_{SN}$

and  $\zeta_{acc,0}$ , respectively. In contrast to the cases with different  $f_{in}$ , the effects of the variations of these two parameters are prominent at a late stage of evolution as expected from the discussion in the previous paragraph. SN destruction decreases and accretion increase the dust emission relative to the stellar emission as expected. Thus, we conclude that SN destruction and dust accretion are important when the system is enriched with dust and metals. We will characterize the metallicity level at which these processes, especially accretion, become dominant in Section 4.3.

Metallicity is often used as a measure for the evolutionary stage of a galaxy. In Fig. 1, we show the evolution of metallicity as a function of  $t/\tau_{SF}$ . We observe that the metallicity reaches  $0.1 Z_\odot$  at  $t/\tau_{SF} = 0.15$ . According to the theoretical calculations by Mancini et al. (2015), the metallicity of the LBGs is less than  $0.1 Z_\odot$ . Therefore, we first put a constraint on the metallicity as  $Z < 0.1 Z_\odot$ . Since the galaxies detected by ALMA may be biased to evolved ones as we discuss later, we also examine a case where we do not put any constraint on the metallicity.

### 3.2 Constraint on the dust evolution parameters

The dust evolution parameters ( $f_{in}, \zeta_{acc,0}, \zeta_{SN}$ ) are constrained by the condition that the observed  $\nu f_{d,\nu}/f_{UV}$  is achieved. This condition is written as

$$\max(\nu f_{d,\nu}/f_{UV})_{\text{model}} \geq (\nu f_{d,\nu}/f_{UV})_{\text{obs}}, \quad (14)$$

where the subscripts ‘model’ and ‘obs’ denote the calculated and observed values, respectively, and max is the maximum value over the galaxy lifetime.

Before analyzing the result, we first discuss the probable ranges of the three parameters ( $f_{in}, \zeta_{acc,0}, \zeta_{SN}$ ). As compiled in Kuo et al. (2013), the value of the condensation efficiency  $f_{in}$  expected from theoretical calculations has large uncertainty. Thus, we investigate the value from 0.01 to 0.5 with  $f_{in} = 0.1$  being the fiducial value. Also, McKee (1989) and Lisenfeld & Ferrara (1998) show that  $\beta_{SN} = M_g/(\tau_{SN}\psi) = \tau_{SF}/\tau_{SN}$  (which is equivalent with  $1/\zeta_{SN}$  in our paper) is  $\approx 10$ . For a wide parameter survey, we investigate the range  $0.01 \lesssim \zeta_{SN} \lesssim 1$ . We are interested in as efficient accretion as suggested by Mancini et al. (2015). To consider such efficient accretion, we focus on  $\zeta_{acc,0}$  down to  $10^{-4}$  (see also the discussion in Section 4.1).

In the upper panel of Fig. 2, we show the area on the  $(\zeta_{acc,0}, \zeta_{SN})$  plane in which the set of  $(f_{in}, \zeta_{acc,0}, \zeta_{SN})$  of A1689-zD1 satisfies the above condition (equation 14) at  $Z < 0.1 Z_\odot$  (expected metallicity for LBGs by Mancini et al. 2015). We find that for  $f_{in} \lesssim 0.1$ ,  $\zeta_{acc,0}$  much smaller than  $\zeta_{SN}$  is necessary to explain the observational data. This is because only when the accretion time-scale is shorter than the supernova time-scale, the dust could have chance to grow before being destroyed by SNe. If we assume a standard value of  $\zeta_{SN} \sim 0.1$  as suggested for nearby galaxies (McKee 1989), small values of  $\zeta_{acc,0}$  ( $< 0.004$ ) are required. For large  $f_{in} > 0.5$ , however, the constraint on  $\zeta_{acc,0}$  is not stringent since the dust produced by stellar sources makes it easier to increase  $\nu f_{d,\nu}/f_{UV}$  up to the observed value regardless of accretion. Nevertheless, even for  $f_{in} = 0.5$ , we need  $\zeta_{acc,0} < 0.01$  if SN destruction is efficient ( $\zeta_{SN} \lesssim 0.05$ ). As we discuss later, theoretical dust condensation calculations indicate that  $f_{in}$  is likely to be less than



**Table 1.** Galaxy sample at  $z > 6$  adopted.

Galaxies	redshift	$\nu(1+z)$ (Hz)	$f_{d,\nu}$ (mJy)	$R$ (kpc)	$L_{UV}$ ( $L_{\odot}$ )	Ref. <sup>a</sup>
A1689-zD1	$7.5 \pm 0.2$	$1.9 \times 10^{12}$	$0.066 \pm 0.013$ <sup>b</sup>	0.7	$1.8 \times 10^{10}$ <sup>b</sup>	1
CLM1	$6.17 \pm 0.0003$	$1.9 \times 10^{12}$	$0.044 \pm 0.026$ <sup>c</sup>	2.65	$3.61 \times 10^{10}$	2

*Note.*

<sup>a</sup> References 1) Watson et al. (2015). 2) Willott et al. (2015).

<sup>b</sup> Corrected for the gravitational lensing, magnification by a factor 9.3.

<sup>c</sup> Neglected the low gravitational magnification 1.13.

0.5, which means that dust growth by accretion is important to explain the dust emissions detected by ALMA for A1689-zD1.

Next we remove the condition for the metallicity in the lower panel of Fig. 2 by allowing a possibility that LBGs detected by ALMA are more metal-rich than expected (i.e.  $Z > 0.1 Z_{\odot}$ ). We can see that the trend of  $f_{in} = 0.5$  barely changes, meaning that the large efficiency of stellar dust production produces a sufficient amount of dust in the early phase of evolution as shown in Fig. 1a. In contrast, the condition for  $\zeta_{acc,0}$  is much more relaxed for  $f_{in} = 0.01$  and 0.1. This means that allowing for a metal-rich stage is essential for accretion, since the efficiency of accretion is proportional to the metallicity. As shown later,  $\zeta_{acc,0} \sim 0.1$  is similar to the value inferred for nearby galaxies. Thus, if the LBGs detected by ALMA at  $z > 6$  are solar-metallicity objects, their rich dust content can be explained by assuming an accretion efficiency expected for nearby galaxies.

The upper and lower panel of Fig. 3 show the results for CLM1. Comparing Figs. 2 and 3, we observe that the condition for dust formation and SN destruction is similar for both objects. That is, for small dust condensation efficiency in stellar ejecta ( $f_{in} \lesssim 0.1$ ), both object need very efficient dust accretion ( $\zeta_{acc,0} \lesssim 0.004$ ) under the metallicity constraint  $Z < 0.1 Z_{\odot}$ . This constraint on the accretion time-scale is much relaxed if we allow the metallicity to be higher than  $0.1 Z_{\odot}$ . The fact that we obtain very similar constraints for both objects indicates that detection of LBGs by ALMA requires a similar range for ( $f_{in}$ ,  $\zeta_{acc,0}$ ,  $\zeta_{SN}$ ).

## 4 DISCUSSION

### 4.1 Likely values for the parameters

Knudsen et al. (2016) derived the SFR of A1689-zD1 as  $12 M_{\odot} \text{ yr}^{-1}$  from the submm continuum. Although the gas has not been detected, Watson et al. (2015) derived a gas mass as  $2 \times 10^9 M_{\odot}$  based on the Schmidt-Kennicutt law, which is equivalent to assuming a star formation time-scale of  $1.7 \times 10^8 \text{ yr}$ . Mancini et al. (2015) showed, using their semi-analytic models of galaxy formation and evolution, that A1689-zD1 requires very short accretion time-scale,  $\tau_{acc,0} = 0.2 \text{ Myr}$ . Thus, the literature value indicates that  $\zeta_{acc,0} \sim 1.2 \times 10^{-3}$ . Our constraint obtained in Fig. 2 shows  $\zeta_{acc,0} \lesssim 4 \times 10^{-3}$  if we impose the metallicity constraint  $Z < 0.1 Z_{\odot}$  as indicated by Mancini et al. (2015). Thus, we confirm their conclusion about the necessity of strong accretion quantitatively (see also Michałowski 2015). Such a

high accretion efficiency is realized if the molecular clouds are very dense (Kuo et al. 2013; Schneider et al. 2016). However, we also show that if we allow larger metallicities, we obtain  $\zeta_{acc,0} \lesssim 5 \times 10^{-2}$  with  $f_{in} = 0.1$  and  $\zeta_{SN} = 0.1$ . If we adopt the above star formation time-scale, this corresponds to  $\tau_{acc,0} \sim 8.5 \times 10^6 \text{ yr}$ , which is consistent with the accretion time-scale derived for nearby galaxies (Hirashita & Kuo 2011). Note that the dust emission is only tentatively detected for CLM1. In other words, the detection of dust continuum by ALMA at  $z \gtrsim 6$  indicates that the object should satisfy either of the following conditions: (i) very efficient condensation in stellar ejecta ( $f_{in} \gtrsim 0.5$ ), (ii) very efficient dust growth by accretion with  $\zeta_{acc,0} \lesssim 4 \times 10^{-3}$ , or (iii) high metallicity ( $\gtrsim$  solar metallicity).

Recently, Ferrara et al. (2016) proposed another reason for the ‘deficit’ of dust emission for high- $z$  LBGs. Since the ISM in high- $z$  galaxies has a high pressure, high- $z$  LBGs host dense molecular clouds (Pallottini et al. 2016). Thus, a large fraction of dust is ‘hidden’ in the shielded environment of the dense molecular clouds. Since such a hidden component of dust has dust temperatures as low as the CMB temperature at the redshift of the LBGs, its far-infrared emission is weak. If this deficit of dust emission is common for high- $z$  LBGs, more extreme conditions (i.e. higher efficiencies) for dust enrichment than shown in this paper would be necessary for ALMA detection of dust emission.

The above conditions for ALMA detection may be modified if we consider gas inflow and outflow from galaxies. We adopted a closed-box model in this paper for simplicity. As mentioned at the beginning of Section 2.1, if we include the effect of inflow and outflow, we need to consider the dilution of metals and dust (Feldmann 2015). However, if we define the total baryonic mass available in the end as  $M_0$  and define the star formation time-scale by the total gas mass including what the galaxy obtain in its entire lifetime, we could use the same framework. Moreover, we have confirmed that we obtain a similar constraint on the accretion time-scale to that obtained by Mancini et al. (2015), who took into account the build-up of galaxy mass. Thus, we expect that our conclusion does not change significantly even if we take into account realistic gas inflow and outflow that occur in the course of galaxy evolution.

### 4.2 Dependence on grain properties

Our model assumes dust properties such as the grain radius  $a$ , the dust material density  $s$ , the emissivity index  $\beta$ , and the mass absorption coefficient at  $158 \mu\text{m}$   $\kappa_{158}$ . Here we in-

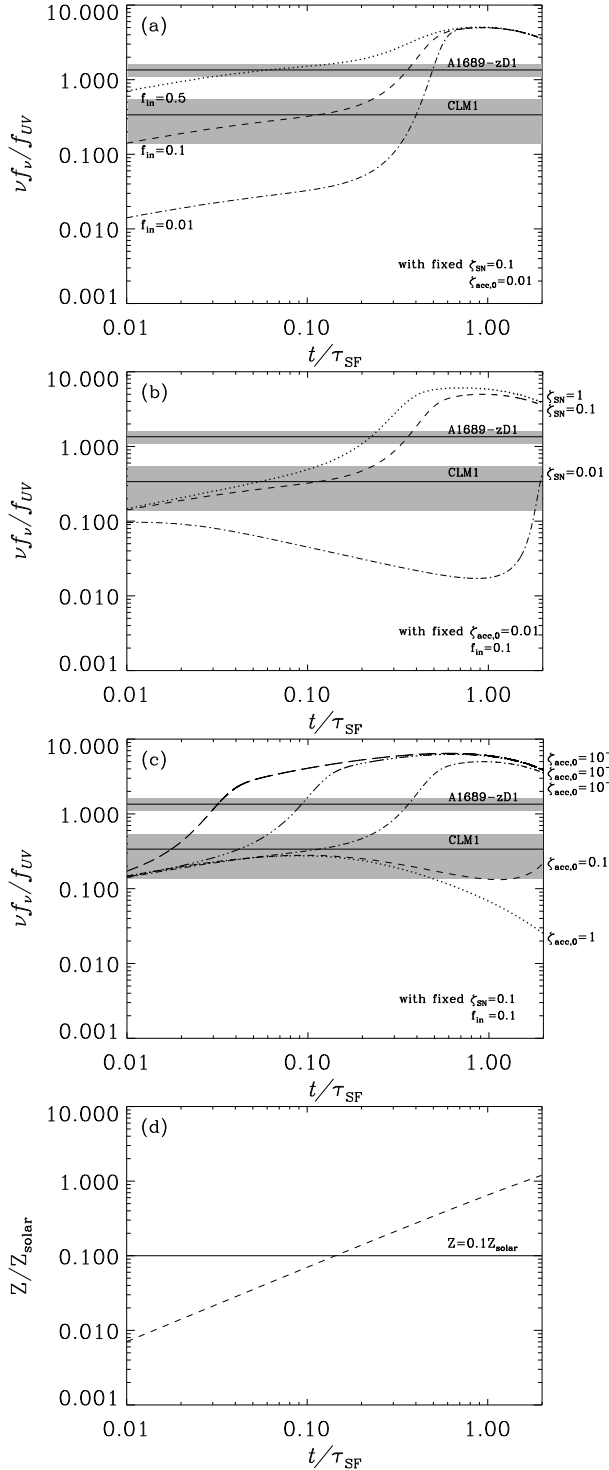


**Figure 1.** Normalized dust emission flux  $\nu f_\nu/f_{UV}$  as a function of the normalized time  $t/\tau_{SF}$ . The horizontal lines at  $\nu f_\nu/f_{UV} = 1.35$  and  $0.34$  are the observed values of A1689-zD1 and CLM1, respectively. The shaded area shows the error of each object. (a) The dotted, dashed, and dotted-dashed lines show the results for  $f_{in} = 0.5, 0.1$ , and  $0.01$ , respectively, with  $\zeta_{SN} = 0.1$  and  $\zeta_{acc,0} = 0.01$ . (b) The dotted, dashed, and dotted-dashed lines are for  $\zeta_{SN} = 1, 0.1$  and  $0.01$ , respectively, with  $\zeta_{acc,0} = 0.01$  and  $f_{in} = 0.1$ . (c) The long-dashed, tripple-dotted-dashed, dotted-dashed, dashed and dotted lines are for  $\zeta_{acc,0} = 10^{-4}, 10^{-3}, 0.01, 0.1$ , and  $1$ , respectively with  $\zeta_{SN} = 0.1$  and  $f_{in} = 0.1$ . (d) Metallicity evolution (dotted line). The horizontal solid line shows  $Z = 0.1 Z_\odot$ : LGBs at  $z > 6$  typically have metallicities below this level (Mancini et al. 2015).

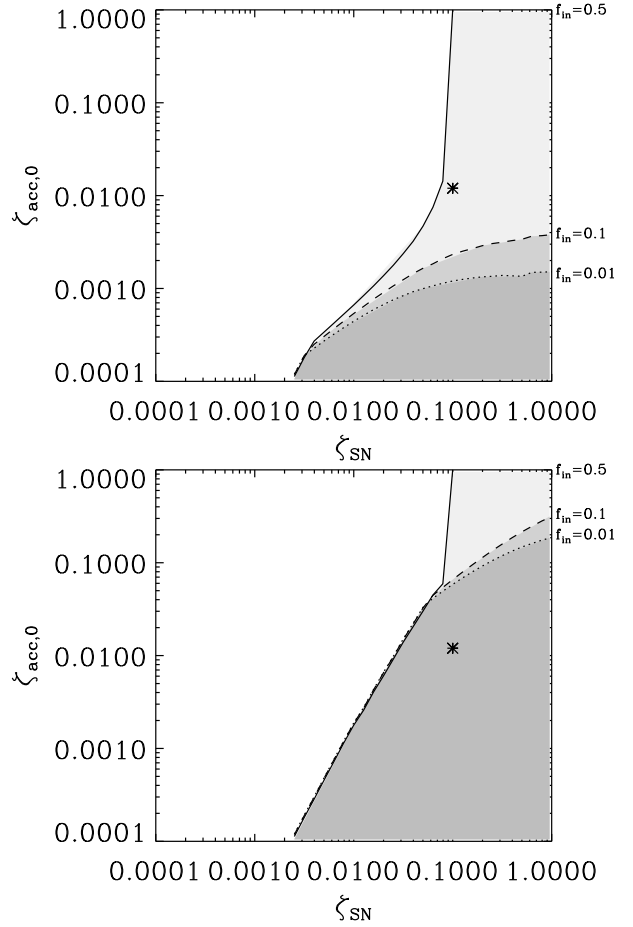


**Figure 2.** Ranges of the time-scale parameters for accretion and SN destruction ( $\zeta_{acc,0}, \zeta_{SN}$ ) constrained by A1689-zD1 for  $f_{in} = 0.5, 0.1$ , and  $0.01$ . The region on the right and lower side (shaded region) of each line satisfies the criterion. The solid, dashed, and dotted lines are the boundary lines for  $f_{in} = 0.5, 0.1$ , and  $0.01$ , respectively. The upper and lower panel are with and without the criterion of metallicity  $Z > 0.1 Z_\odot$ , respectively. The asterisk refers to the standard accretion and destruction values of nearby galaxies,  $(\zeta_{acc,0}, \zeta_{SN}) = (0.012, 0.1)$

investigate how much the constraints obtained for the parameters (such as shown in Fig. 2) are affected by the assumed dust properties. Since similar results are obtained for both galaxies, we concentrate on A1689-zD1 in this subsection. We also fix the value of  $f_{in}$  to  $0.1$ .

A larger grain radius leads to a more efficient emission, thus, a lower temperature (see equation 10; the emission scales with  $a^3$  while the absorption scales with  $a^2$ ). Thus, we may obtain a severer constraint on the parameters for a larger grain. We here investigate the case of  $a = 1 \mu m$  in Fig. 4a. We find that the constraints on  $\zeta_{acc,0}$  and  $\zeta_{SN}$  differ only by a factor of  $\sim 2$  between  $a = 0.1 \mu m$  and  $1 \mu m$ .

Variation of the dust material affects the values of  $s$ ,  $\beta$ , and  $\kappa_{158}$ . For the dust material, we adopted graphite above, but we here investigate other grain species listed as possible dust species by Hirashita et al. (2014); silicate, amorphous carbon (AC),  $SN_{con}$  (theoretically expected dust material properties for condensation in supernova ejecta; Nozawa et al. (2003)) and  $SN_{des}$  (theoretically expected val-

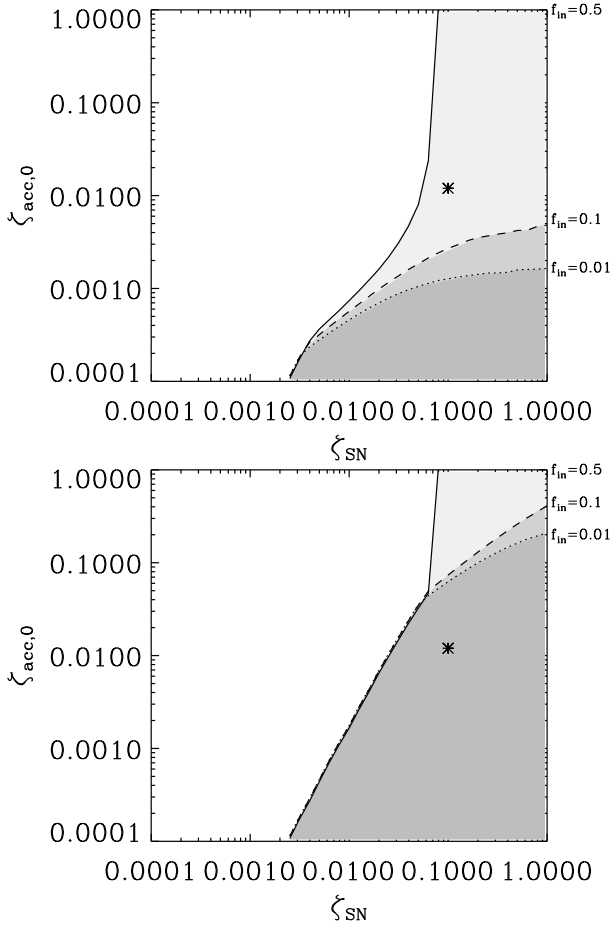


**Figure 3.** Same as Fig. 2 but for the other object, CLM1.

ues with reverse shock destruction in a supernova remnant; Nozawa et al. (2007)). The dust properties are summarized in Table 2. The constraints obtained for each grain species are compared in Fig. 4b. The longest accretion time-scale is allowed for AC among all the species, since AC has the highest emissivity, thus achieving the observed ALMA flux most easily. For the opposite reason, SN<sub>con</sub> requires the shortest accretion time-scale.

### 4.3 Importance of metallicity measurements

In the above, two solutions were broadly permitted to explain the observed dust abundance in the two high- $z$  galaxies. One is an extremely high condensation efficiency  $f_{in}$  typically  $\geq 0.5$ , although this solution is not supported by theoretical condensation calculations, and the other is an efficient accretion. As shown in Asano et al. (2013), the rise of dust abundance occurs after the system is enriched with metals to a certain ‘critical’ metallicity, since efficient accretion occurs only when a sufficient amount of accreting materials (i.e. metals) is available.

Now we reformulate the critical metallicity, which is estimated by equating the dust formation rates of stellar sources and accretion, i.e. the second and the fourth terms on the right-hand side of equation (3). The solution gives the critical metallicity in the sense that, if the metallicity

**Table 2.** Dust properties.

Species	$\kappa_{158}^a$ ( $\text{cm}^2 \text{g}^{-1}$ )	$\beta^b$	$s^c$ ( $\text{g cm}^{-3}$ )	Ref. <sup>d</sup>
Graphite	20.9	2	2.26	1, 2
Silicate	13.2	2	3.3	1, 2
SN <sub>con</sub> <sup>e</sup>	5.57	1.6	2.96	3
SN <sub>dest</sub> <sup>f</sup>	8.94	2.1	2.48	4
AC <sup>g</sup>	28.4	1.4	1.81	5, 6

<sup>a</sup>Mass absorption coefficient at 158  $\mu\text{m}$ .

<sup>b</sup>Emissivity index ( $\kappa_\nu \propto \nu^\beta$ ).

<sup>c</sup>Material density.

<sup>d</sup>References: 1) Draine & Lee (1984); 2) Dayal, Hirashita, & Ferrara (2010); 3) Hirashita et al. (2005); 4) Hirashita et al. (2008); 5) Zubko et al. (1996); 6) Zubko et al. (2004).

<sup>e</sup>Dust condensed in SNe before reverse shock destruction (Nozawa et al. 2003).

<sup>f</sup>Dust ejected from SNe after reverse shock destruction (Nozawa et al. 2007).

<sup>g</sup>Amorphous carbon.

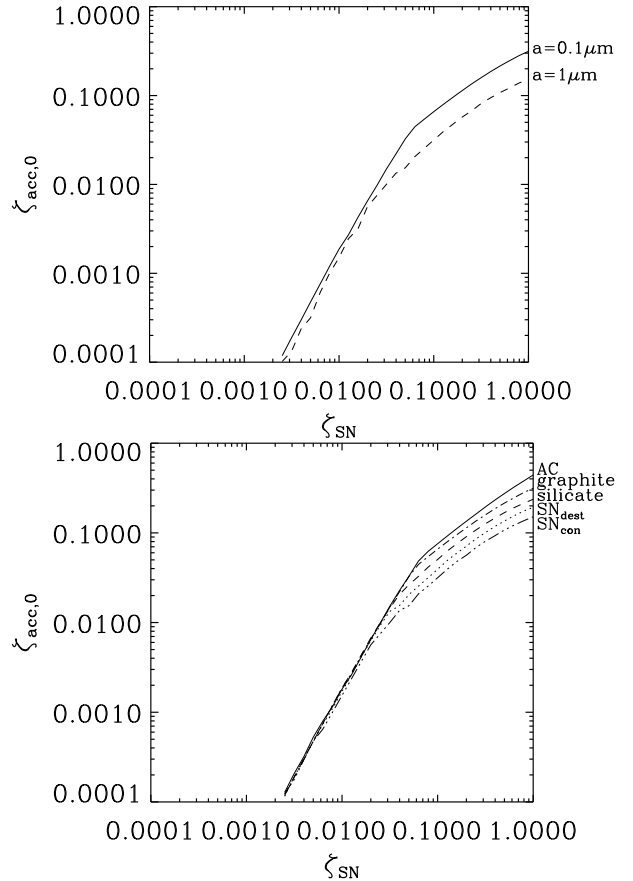


**Figure 4.** Same as Fig. 2 but for various grain radii and material properties. Only the boundary for  $f_{in} = 0.1$  is shown. Upper panel: Grain size dependence. The solid and dashed lines refer to  $a = 0.1$  and  $1 \mu\text{m}$ , respectively. Lower panel: Dust material dependence. The lines from top to bottom refer to AC, graphite, silicate, SN<sub>dest</sub>, and SN<sub>con</sub>, respectively.

is higher than this, accretion is the dominant mechanism of dust production over stellar dust production. As a consequence, we obtain the critical metallicity as (see Appendix for the derivation)

$$\left(\frac{Z}{Z_{\odot}}\right)_{\text{cr}} \simeq \zeta_{\text{acc},0}^{1/2}, \quad (15)$$

where the subscript ‘cr’ indicates that this metallicity gives the critical metallicity for accretion (see also [Feldmann \(2015\)](#)).

Under the metallicity constraint  $Z < 0.1 Z_{\odot}$ , values of  $\zeta_{\text{acc},0}$  smaller than  $4 \times 10^{-3}$  appropriate for the sample of  $z > 6$  galaxies indicate that the critical metallicity is  $\sim 0.06 Z_{\odot}$ . Therefore, if we find that the metallicity is  $0.06 Z_{\odot} < Z < 0.1 Z_{\odot}$ , it would strongly supports the scenario of efficient dust growth by accretion in those galaxies. Otherwise, for  $Z < 0.06 Z_{\odot}$ , efficient stellar dust production would be the way to explain the dust emission detected by ALMA. Taking away the metallicity constraint, we obtained a constraint  $\zeta_{\text{acc},0} \lesssim 0.1$  (i.e. a similar efficiency of accretion to the one in nearby galaxies) for  $\zeta_{\text{SN}} \sim 0.1$ , leading to a critical metallicity of  $\sim 0.3 Z_{\odot}$ . Thus, if the metallicity is proves to be larger than  $0.3 Z_{\odot}$ , accretion naturally explains the high dust luminosity, but it is not necessary to assume an extremely high accretion efficiency compared with the one in nearby galaxies.

It is generally difficult to detect metal emission lines for galaxies at  $z \gtrsim 6$ . [Nagao et al. \(2012\)](#) proposed to use far infrared fine structure lines to assess the metallicity. Future sensitive submm observations may constrain the metallicities in high- $z$  LBGs. Alternatively, the grain size distribution would serve to constrain the dominant dust production process, since the dust grains produced by stars have large sizes ( $\approx 0.1 \mu\text{m}$ ), while there should be a large abundance of small grains produced by shattering if dust growth by accretion is actively occurring ([Asano et al. 2013](#)). Probably, extinction curves, although they are not easy to be derived, could provide the information on the grain size distribution ([Asano et al. 2014](#)). Observations of dense molecular gas would directly probe the existence of clouds hosting dust growth by accretion, since extremely dense molecular clouds may enhance the efficiency of dust growth ([Kuo et al. 2013](#)). Indeed, [Pallottini et al. \(2016\)](#) showed in their simulation a dense and metal-enriched region in the central part of an LBG. Such a dense region may host dust growth. Observations of highly excited molecular line whose critical density is high may serve to identify such a dense region ([Vallini et al. 2016](#)). Thus, if observations of dense molecular clouds prove that molecular clouds are dense (by high excitation molecular lines, etc.), they would support the possibility of efficient accretion.

## 5 CONCLUSION

Recent ALMA observations have started to detect normal galaxies even at  $z > 6$ . We investigated what constraint we can get for the dust enrichment in normal  $z > 6$  galaxies detected by ALMA. To this aim, we used a theoretical model that includes major processes driving dust evolution in a galaxy, including dust condensation in stellar ejecta, dust growth by the accretion of gas-phase metals, and supernova

destruction. To cancel out unknown quantities such as the total baryonic content and the star formation time-scale, we consider the flux at the ALMA band normalized to the UV flux as a function of time normalized to the star formation time-scale. Using the observational data for A1689-zD1 and CLM1, we obtained the range of the time-scales (or efficiencies) of the above mentioned processes by examining if the observed level of the ALMA flux normalized to the UV flux is achieved. We find that if we assume extremely high condensation efficiency in stellar ejecta ( $f_{\text{in}} \gtrsim 0.5$ ), star-dust may be enough to explain the observed ALMA flux in their early evolutionary stage, unless dust destruction by supernovae in those galaxies is stronger than that in nearby galaxies. If we assume a condensation efficiency expected from theoretical calculations ( $f_{\text{in}} \lesssim 0.1$ ), dust growth by accretion is required. If the metallicities of those objects are lower than  $0.1 Z_{\odot}$  as suggested by a previous theoretical model ([Mancini et al. 2015](#)), strong dust growth (ten times stronger than assumed for nearby galaxies) is derived. Alternatively, if we allow for solar metallicity, only moderate accretion whose efficiency is comparable to that in nearby galaxies is required to explain the ALMA detections. These results indicate that the normal galaxies detected by ALMA at  $z > 6$  are biased to objects (i) with high dust condensation efficiency in stellar ejecta, (ii) with strong dust growth, or (iii) with efficient dust growth because of fast metal enrichment up to solar metallicity. We finally argue that measurement of metallicity will provide a key to distinguishing among these possibilities.

## ACKNOWLEDGMENT

We are grateful to the anonymous referee for useful comments. HH thanks the Ministry of Science and Technology for support through grant MOST 105-2112-M-001-027-MY3.

## REFERENCES

- Aravena M., et al., 2016, preprint
- Asano R. S., Takeuchi T. T., Hirashita H., Inoue A. K., 2013, *Earth, Planets, and Space*, **65**, 213
- Asano R. S., Takeuchi T. T., Hirashita H., Nozawa T., 2014, *MNRAS*, **440**, 134
- Bianchi S., Schneider R., 2007, *MNRAS*, **378**, 973
- Bouvens R., et al., 2016, preprint, ([arXiv:1606.05280](#))
- Capak P. L., et al., 2015, *Nature*, **522**, 455
- Carroll S. M., Press W. H., Turner E. L., 1992, *ARA&A*, **30**, 499
- da Cunha E., et al., 2013, *ApJ*, **766**, 13
- Dayal P., Hirashita H., Ferrara A., 2010, *MNRAS*, **403**, 620
- de Bennassuti M., Schneider R., Valiante R., Salvadori S., 2014, *MNRAS*, **445**, 3039
- Dwek E., 1998, *ApJ*, **501**, 643
- Dwek E., Scalo J. M., 1980, *ApJ*, **239**, 193
- Feldmann R., 2015, *MNRAS*, **449**, 3274
- Ferrara A., Hirashita H., Ouchi M., Fujimoto S., 2016, preprint
- Gall C., Andersen A. C., Hjorth J., 2011, *A&A*, **528**, A13
- Gould R. J., Salpeter E. E., 1963, *ApJ*, **138**, 393
- Hirashita H., 1999, *ApJ*, **510**, L99
- Hirashita H., Kuo T.-M., 2011, *MNRAS*, **416**, 1340
- Hirashita H., Ferrara A., Dayal P., Ouchi M., 2014, *MNRAS*, **443**, 1704
- Inoue A. K., 2003, *PASJ*, **55**, 901
- Inoue A. K., 2011, *Earth, Planets, and Space*, **63**, 1027



- Knudsen K. K., Watson D., Frayer D., Christensen L., Gallazzi A., Michałowski M. J., Richard J., Zavala J., 2016, preprint, ([arXiv:1603.03222](#))
- Kozasa T., Hasegawa H., Nomoto K., 1989, *ApJ*, **344**, 325
- Kuo T.-M., Hirashita H., Zafar T., 2013, *MNRAS*, **436**, 1238
- Lisenfeld U., Ferrara A., 1998, *ApJ*, **496**, 145
- Maiolino R., et al., 2015, *MNRAS*, **452**, 54
- Mancini M., Schneider R., Graziani L., Valiante R., Dayal P., Maio U., Ciardi B., Hunt L. K., 2015, *MNRAS*, **451**, L70
- Mattsson L., Andersen A. C., 2012, *MNRAS*, **423**, 38
- McKee C., 1989, in Allamandola L. J., Tielens A. G. G. M., eds, IAU Symposium Vol. 135, Interstellar Dust. p. 431
- Michałowski M. J., 2015, *A&A*, **577**, A80
- Nagao T., Maiolino R., De Breuck C., Caselli P., Hatsukade B., Saigo K., 2012, *A&A*, **542**, L34
- Nozawa T., Kozasa T., Umeda H., Maeda K., Nomoto K., 2003, *ApJ*, **598**, 785
- Nozawa T., Kozasa T., Habe A., 2006, *ApJ*, **648**, 435
- Nozawa T., Kozasa T., Habe A., Dwek E., Umeda H., Tominaga N., Maeda K., Nomoto K., 2007, *ApJ*, **666**, 955
- Ota K., et al., 2014, *ApJ*, **792**, 34
- Ouchi M., et al., 2013, *ApJ*, **778**, 102
- Pallottini A., Ferrara A., Gallerani S., Vallini L., Maiolino R., Salvadori S., 2016, preprint, ([arXiv:1609.01719](#))
- Rémy-Ruyer A., et al., 2014, *A&A*, **563**, A31
- Schaerer D., Boone F., Zamojski M., Staguhn J., Dessauges-Zavadsky M., Finkelstein S., Combes F., 2015, *A&A*, **574**, A19
- Schneider R., Hunt L., Valiante R., 2016, *MNRAS*, **457**, 1842
- Tinsley B. M., 1980, *Fund. Cosmic Phys.*, **5**, 287
- Todini P., Ferrara A., 2001, *MNRAS*, **325**, 726
- Valiante R., Schneider R., Salvadori S., Bianchi S., 2011, *MNRAS*, **416**, 1916
- Vallini L., Ferrara A., Pallottini A., Gallerani S., 2016, preprint, ([arXiv:1606.08464](#))
- Watson D., Christensen L., Knudsen K. K., Richard J., Gallazzi A., Michałowski M. J., 2015, *Nature*, **519**, 327
- Willott C. J., Carilli C. L., Wagg J., Wang R., 2015, *ApJ*, **807**, 180
- Yajima H., Shlosman I., Romano-Díaz E., Nagamine K., 2015, *MNRAS*, **451**, 418
- Zhukovska S., Gail H.-P., Tieloff M., 2008, *A&A*, **479**, 453

## APPENDIX A: CRITICAL METALLICITY FOR DUST GROWTH BY ACCRETION

We compare the two dust-supplying mechanisms, dust formation by stellar sources and dust growth by accretion. The rates of these two dust formation paths are represented by the second and the fourth terms in equation (3). Because of the dependence on metallicity, dust growth by accretion becomes dominated over stellar dust production at a certain metallicity referred to as the critical metallicity. This critical metallicity is obtained by equating the above two terms as

$$f_{\text{in}} \mathcal{V}_Z \psi \sim \frac{M_d}{\tau_{\text{acc},0}} \frac{Z}{Z_{\odot}}, \quad (\text{A1})$$

where we adopted  $1 - f_Z \sim 1$ , which holds unless  $f_{\text{in}}$  is nearly unity, for simplicity. We further use some basic relations,  $\tau_{\text{SF}} = M_g / \psi$ ,  $\mathcal{D} = M_d / M_g$ , and  $\zeta_{\text{acc},0} = \tau_{\text{acc},0} / \tau_{\text{SF}}$ , and apply the solution of pure stellar dust production,  $\mathcal{D} \sim f_{\text{in}} Z$ , which is still approximately applicable when accretion starts to be dominant over stellar dust production. We also use the fact that the metal yield has a similar value to the solar metallicity (e.g. Tinsley 1980). After all, equation (A1) is

reduced to

$$\left( \frac{Z}{Z_{\odot}} \right) \sim \zeta_{\text{acc},0}^{1/2}. \quad (\text{A2})$$

This metallicity is referred to as the critical metallicity in Section 4.3.

This paper has been typeset from a  $\text{\TeX}/\text{\LaTeX}$  file prepared by the author.